2_C50

CFD Modeling of Room Air Flow Effects on Inactivation of Aerosol SARS-CoV-2 by an Upper Room Ultraviolet Germicidal Irradiation (UVGI) System

Youngbo Won, PhD
Student Member ASHRAE
Donghyun Rim, PhD
Associate Member ASHRAE
Richard Mistrick, PhD
William Bahnfleth, PhD
Presidential Member/Fellow ASHRAE

ABSTRACT

Ultraviolet germicidal irradiation (UVGI) inactivates viral aerosols in indoor environments. Upper room UVGI systems use wall or ceiling mounted fixtures to create a disinfection zone above the occupied zone. The performance of upper room UVGI systems varies with indoor airflow induced by mechanical ventilation and thermal plumes from occupants, which carries contaminated air into the disinfection zone where viral aerosols are partially inactivated before circulating back into the breathing zone. This study used computational fluid dynamics (CFD) modeling to investigate the effect of an upper room UVGI system on spatial distributions of viral aerosols with UV-C susceptibility representative of coronaviruses as a function of ventilation system characteristics. Upper-room UVGI confined elevated viral aerosol concentrations to the vicinity of an infector, while the room average viral aerosol concentration was reduced by two orders of magnitude relative to a case without UVGI. Return air recirculation rates and ventilation strategy (i.e. mixing vs. displacement) had notable effects on the disinfection effectiveness of the UVGI system. For mixing ventilation, as the recirculation air flow rate increased from 0 to 5.3 h^{-1} with a fixed outdoor air flow of 0.7 h^{-1}, UVGI inactivation escalated by 62%. Mixing ventilation at 0.7 h^{-1} without recirculation in the room with a volume of 108 m^3 was 30% more effective in inactivating airborne viruses than displacement ventilation, due to the higher air mixing.

INTRODUCTION

COVID-19 (coronavirus disease 2019), caused by the SARS-CoV-2 virus, developed into a global pandemic during 2020, resulting in 138 million cases and 3 million deaths as of April 15, 2021("WHO Coronavirus (COVID-19) Dashboard" n.d.). Respiratory viruses, including SARS-CoV-2, are shed by an infector when breathing, talking, singing, sneezing, or coughing and transported by viral droplet or viral aerosol to receptors (susceptible individuals) (Prather, Wang, and Schooley 2020). Disease transmission can occur via inhalation, deposition of larger droplets in the eyes, nose, or mouth, and also by fomite (intermediate surface) transmission. The viral particle concentrations are non-uniformly distributed near infectors and are affected by indoor airflow (Zhang and Chen 2009).

Ultraviolet germicidal irradiation (UVGI) can be utilized to reduce virus transmission in indoor environments, where most airborne disease transmission occurs (Nishiura et al. 2020). Ultraviolet light in the UV-C wavelength

Youngbo Won is a post-doc researcher, **Donghyun Rim** and **Richard Mistrick** are associate professors, and **William Bahnfleth** is a professor in the Department of Architectural Engineering, Penn State University, University Park, PA, USA.

band, damages the DNA and RNA of microorganisms by breaking bonds between base pairs, preventing them from reproducing. A common application of UVGI is in a so-called upper room system. The systems are placed above the occupied zone to create a disinfection zone in which the microorganisms carried in aerosols are inactivated. A study (Kowalski 2010) shows that compared to ventilation that dilutes microbial aerosol with outdoor air, upper room UVGI is more efficient in inactivating microbial pathogens including viruses. A previous study (Riley and Nardell 1990) shows that the first-order removal rate of a microbial species by UVGI is equivalent to the outdoor ventilation rates of 20 - 80 h^{-1}.

Since heating, ventilation, and air-conditioning (HVAC) air flows can transport the infectious aerosols to the disinfection zone of an upper room UVGI system, while ventilation strategy and outdoor air flow rate can influence their performance. An experimental study (Nunayon, Zhang, and Lai 2020) showed that UVGI in a well-mixed room increases performance 50-80% compared to a poorly-mixed room. However, only a few studies are available on upper room UVGI performance against coronaviruses under representative ventilation conditions (Zhu et al. 2014; Xu et al. 2017). To address this knowledge gap, the objective of the study is to examine spatial distributions of viral aerosols exhaled from an infector and investigate how indoor ventilation conditions affect the performance of upper room UVGI systems.

METHOD

A CFD model was developed to examine the effects of an upper room UVGI system on spatial distributions of viral aerosol and viral aerosol removal rate under steady-state conditions in a parametric study using Star-CCM+.

The CFD model geometry

Figure 1 shows the geometry of the modeled indoor space and air distribution. The plan dimensions of the space were 6 m by 6 m and the ceiling height was 3 m, giving a volume of 108 m^3. Four occupants were located in the room, one infector and three receptors. The surface temperatures were set to 35 ºC for the surface of occupants and 25 ºC for the other indoor surfaces. As outdoor air flow rate changes from 0.7 h^{-1} to 6 h^{-1}, the outdoor air temperature varies from 19.1 to 24.1 ºC to set the indoor air temperature as 25 ºC. Infectious particles were released from the mouth of the infector, which had an opening area of 0.08 m^2 (Gupta, Lin, and Chen 2010). To simulate talking, the exhalation speed of the infector was set to a constant value of 2 m/s (Gupta, Lin, and Chen 2010; Chao et al. 2009). Based on measured data (Noti et al. 2013) for concentrations of particles emitted by an adult, the concentration of viral aerosol emitted from the infector's mouth was set to a volume fraction of 4×10^{-4}. Considering both air flow rate from the infector and volume fraction of particulate matter, the source generation rate is computed as 2.2×10^{-7} g/s. The distance between facing occupants was 2 m, while 3 m from shoulder to shoulder was applied for side-by-side occupants.

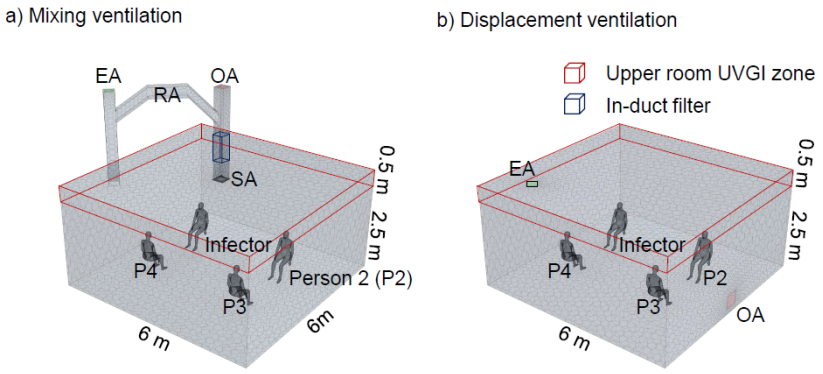

Figure 1 CFD model geometry: (a) mixing ventilation and (b) displacement ventilation. The red box represents the upper room UVGI zone with a first-order decay rate of coronaviruses of 0.124 (s^{-1}).

ASHRAE Standard 62.1 (2019) suggests that the required ventilation rate of office space is 2.5 L/s per person and 0.3 L/s per unit area of 1 m^2. Thus, the ventilation rate of 74.9 m^3/h is calculated for an office area of 36 m^2 with four occupants, which is translated to an air change rate of 0.7 h^{-1}. Both overhead mixing and displacement ventilation were simulated. In the overhead mixing configuration (Fig 1a), recirculated air (RA) in variable amounts was diverted from exhausted air (EA), mixed with outdoor air (OA), and supplied to the indoor space through a 4-way diffuser in the center of the ceiling. In the displacement ventilation case, outdoor air was supplied through a floor-level sidewall diffuser without recirculation (Fig 1b).

An upper room UVGI system was modeled as a 0.5 m deep constant fluence zone beginning 2.5 m above the floor and extending to the ceiling as shown in Figure 1. UV fluence (I) was assumed to be 40 $\mu w/cm^2$, within the range recommended for tuberculosis control systems (Whalen 2009), and the susceptibility constant (k) for the viral aerosol was assumed to be of 0.003 $cm^2/\mu w\text{-}s$, representative of values for coronaviruses, including SARS-CoV-2 virus, giving the first-order decay rate of 0.124 (s^{-1}).

The CFD simulation solved the Eulerian multiphase transport equation, which accounted for dispersed-continuous phase interactions. Dispersed phase viral aerosols were released from the mouth of the infector and distributed in the continuous phase fluid, ambient air. The continuity and conservation equations for mass and energy were solved for each phase by multiplying by the volume fraction. To simulate the turbulent plume around the occupants and in-duct regions, Menter's shear stress transport SST k-ω model was used (Menter 1994).

The concentration of each cell is determined by the balance of convection, diffusion, sources and sinks (E1): (Shiraiwa et al. 2019)

$$\frac{\partial}{\partial t}(\rho M_i) + \frac{\partial}{\partial x_j}(\rho\, u_j M_i) = \frac{\partial}{\partial x_j}\left(\rho\, D_i \frac{\partial M_i}{\partial x_j}\right) + S_i + R_i \qquad \text{(E1)}$$

where ρ is air density; M_i is concentration of viral aerosol; u_j is air velocity; D_i is molecular and turbulent diffusion coefficient; S_i is source term, and R_i is sink term by UVGI inactivation.

Comparison with the well-mixed model (Box model)

The results from the CFD model were compared to values from a well-mixed model (Box model). The room average concentrations and the performances of UVGI were calculated in both models. The performance of UVGI was quantified by computing the equivalent air change rate of the UVGI system. In the box model, the viral aerosol concentration in the room was balanced by ventilation loss, source generation, and the loss due to the UVGI system. The average concentrations of viral aerosols under the steady-state condition were computed using the following equation (E2).

$$C_{avg} = \frac{S}{v(a + kI\gamma)} \qquad \text{(E2)}$$

where C_{avg} (μg cm^{-3}) is a room average concentration of viral aerosol; S (μg h^{-1}) is generation rate of viral aerosol; v (m^3) is the room volume; a (h^{-1}) is air change rate; kI (h^{-1}) is the first-order decay rate by the UVGI system; γ is the ratio of the volume of the UVGI zone to the volume of the room. The volume ratios (γ) are 0.167 for the upper room UVGI system. $kI\gamma$ (h^{-1}) is the equivalent air change of the UVGI.

In the CFD model, the equivalent of the air change rate of the UV system was calculated, based on the room average concentration of viral aerosol using the following equation (E3).

$$kI\gamma = \frac{S}{vC_{avg}} - a \qquad \text{(E3)}$$

Parametric Study

A total of 13 parametric cases were analyzed considering three parameters that affect distributions of viral aerosol and UVGI performance: 1) ventilation strategy, 2) air change rates and recirculation rates, and 3) upper room UVGI system conditions (See Table 1). Cases 1-3 (UVGI on) and 5-7 (UVGI off) have mixing ventilation with 6 h^{-1} of supply air flow and varying outdoor air flow rates. Case 4 also has mixing ventilation, but with 100% outdoor air at the minimum flow rate of 0.7 h^{-1} and UVGI on. Cases 8-10 (UVGI on) and 11-13 are displacement ventilation cases with varying 100% outdoor air supply air flow rates.

Table 1. Parametric study cases

Case	Ventilation strategy	Upper room UVGI	Air flow rate *OA/RA/SA (h^{-1})
1	Mixing	On	0.7/5.3/6
2	Mixing	On	3/3/6
3	Mixing	On	6/0/6
4	Mixing	On	0.7/0/0.7
5	Mixing	Off	0.7/5.3/6
6	Mixing	Off	3/3/6
7	Mixing	Off	6/0/6
8	Displacement	On	0.7/0/0.7
9	Displacement	On	3/0/3
10	Displacement	On	6/0/6
11	Displacement	Off	0.7/0/0.7
12	Displacement	Off	3/0/3
13	Displacement	Off	6/0/6

* OA: outdoor air, RA: return Air, and SA: supply air

RESULTS

Spatial distribution of viral aerosol

Figure 2 shows examples of spatial distributions of viral aerosol concentration for mixing ventilation without (case 5) and with (case 1) UVGI. Figures 2c and 2d are horizontal sections at the height of the occupants' mouths. The virus-containing jet emitted from the mouth of the infector moves away horizontally and upward due to the effects of momentum and buoyancy near the infector and disperses into the ambient air. Due to the effect of mixing ventilation, the viral aerosol is well distributed in the room except near the mouth of the infector. The concentration difference between the mouths of P3 (the farthest located manikin) and P4 (in front of the infector) is less than 10%.

Due to the upper room UVGI system operating (case 1), the average room concentration of viral aerosol was lower by a factor of 151 than without UVGI operation (case 5). Because of the thermal plume, the airflow near the infector transported viral aerosols to the UV irradiation zone before recirculating and dispersing them to the ambient air. Thus, the viral aerosol is only concentrated near the mouth region of occupants.

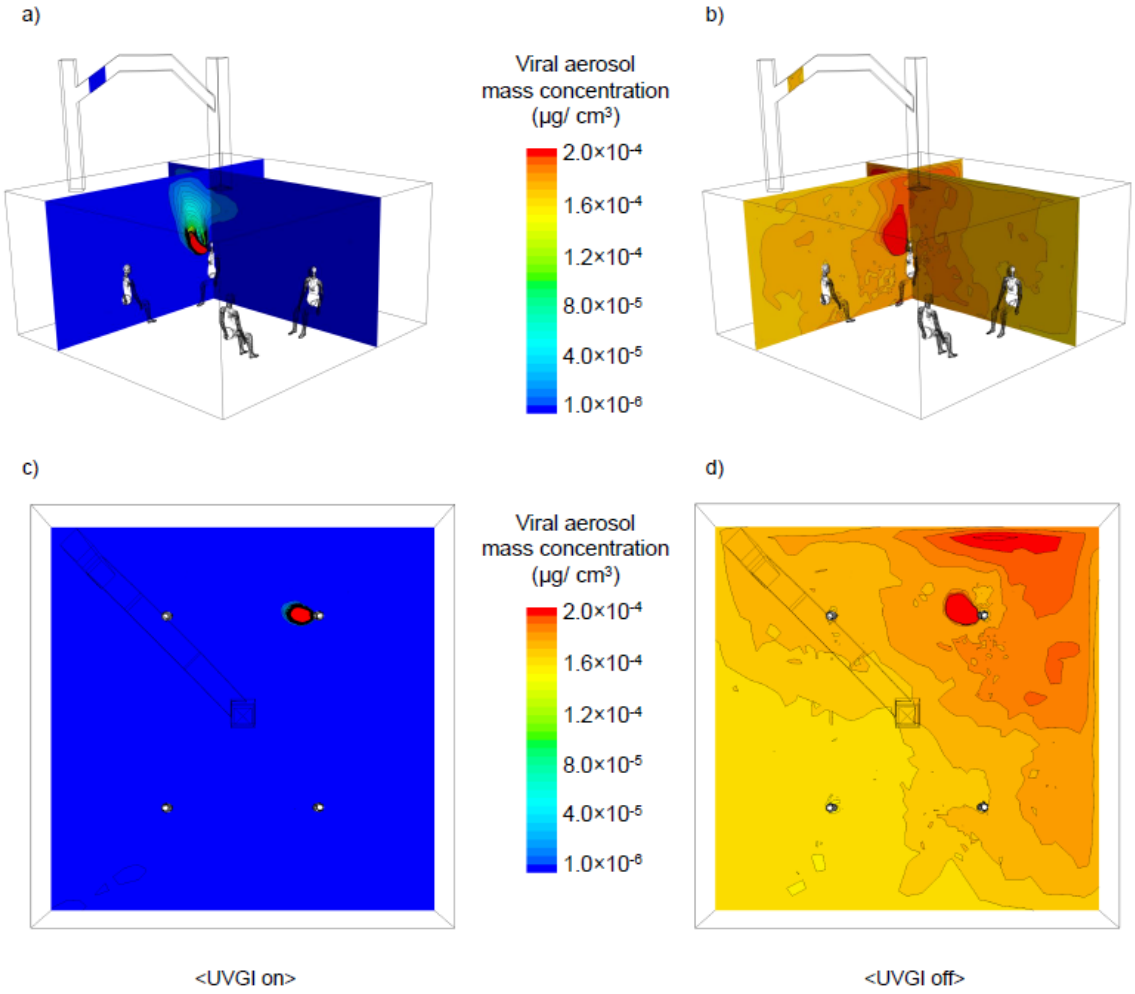

Figure 2 Spatial distributions of viral aerosol concentrations under mixing ventilation condition with an air change rate of 6 h^{-1} (0.7 h^{-1} for OA and 5.3 h^{-1} for RA). The upper room UVGI system is turned off on the left side (case 5), and the system operates on the right side (case 1).

Effects of ventilation strategies on viral aerosol inactivation

Figure 3 shows the effects of ventilation strategies on viral aerosol inactivation rate achieved by the upper room UVGI system. An outdoor air of 0.7 h^{-1} was supplied and the upper-room UVGI system operated in all cases. Air recirculation rate increases UV light exposure time of viral aerosol, resulting in a lower aerosol concentration in a ventilated room. The viral aerosol concentrations at the mouth of P2 - P4 are 1-2 orders of magnitude lower at the higher recirculation rate (5.3 h^{-1}). When the air recirculation rate increases from 0 to 5.3 h^{-1} in the mixing ventilation case, the effective outdoor air change rate of the upper room system increases from 48.7 to 127.2 h^{-1}. Compared to displacement ventilation, mixing ventilation enhanced the performance of the UVGI system. When comparing the age of air in the UVGI zone, the exhaled air under the mixing ventilation condition is six minutes longer in the UVGI zone than displacement ventilation. As a result, the average room concentration under mixing ventilation is 30% lower than that of displacement ventilation under the UVGI operation condition.

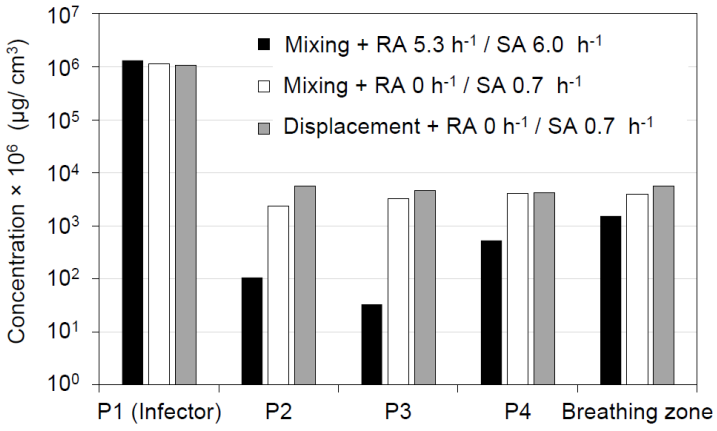

Figure 3 Effects of ventilation strategies (mixing vs. displacement ventilation) and recirculation rates on viral aerosol inactivation rate by the upper-room UVGI system (Cases 1, 4, and 8). Outdoor air of 0.7 h^{-1} is supplied, and the upper-room UVGI system operates in all cases. Concentrations of P1 (infector), P2 (person 2), P3, and P4 are calculated in the mouth regions with an air volume of 0.5 l. The breathing zone is the mean concentration of the ASHRAE breathing zone. RA stands for return air, and SA stands for supply air.

Comparisons of concentrations with the well-mixed model

Figure 4 compares the average concentrations of viral aerosols obtained from the CFD model with the values predicted by the box (well-mixed space) model. In the box model, viral aerosol concentrations were similar regardless of ventilation conditions when the UVGI system operated (see black bars Fig 4a). Because the box model assumes well-mixed conditions, the performance of UVGI was not affected by the airflow, recirculation rate, or infector location. Thus, the viral aerosol removal rate of the UVGI system is equivalent to an air change rate of 64 h^{-1}, showing similar concentrations in all cases. On the other hand, the room average viral aerosol concentrations are influenced by ventilation strategies and recirculation rates in the CFD model, showing the range of 0.001 to 0.006 µg/cm^3. The equivalence air change rate of the UVGI system varies from 48.7 to 132.9 h^{-1} (equivalent ventilation rate: from 1.46 to 3.99 m^3/s) under mixing ventilation conditions, and from 34.1 to 64.5 h^{-1} (equivalent ventilation rate: from 1.02 to 1.94 m^3/s) under displacement ventilation conditions. The CFD result shows mixing ventilation with a higher air mixing rate enhances the UVGI performance.

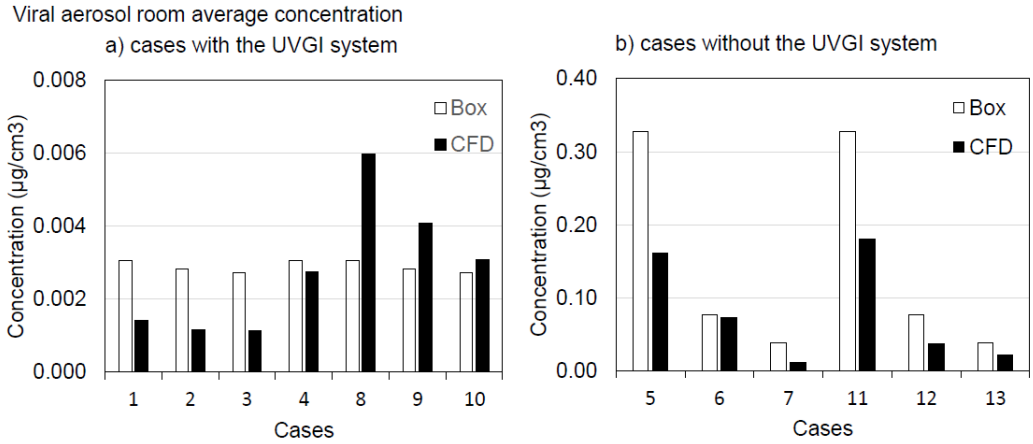

Figure 4 Comparison of average concentrations of viral aerosol between the CFD model and BOX model; a) cases with upper room UVGI and b) cases without upper room UVGI.

DISCUSSION

To reduce viral aerosol transmission, two main strategies are utilized indoors; source control and ventilation (Hult et al. 2015). In general, source control is a more effective way than ventilation. In removing viruses before dispersion under the UVGI operation condition, the impact of transmission to other occupants is lower than using dilution by outdoor air. In places for meeting space, the upper-room UVGI system may be utilized to control sources. The UVGI system effectively disinfects viral aerosols moving upward through buoyancy airflow near the infector before it is dispersed to the ambient air, decreasing 95% of its steady-state concentration.

In this study, the UV fluence was assumed to be uniform throughout the upper room disinfection zone. Actual upper room disinfection systems use wall or ceiling mounted fixtures for which the UV irradiance decreases with distance, so the fluence distribution is non-uniform. The assumption of uniform fluence clearly could affect results, but the fluence value used in this study was typical of the averages for systems recommended by NIOSH. Consideration of the output and light distribution of actual fixtures is important in the design of these systems.

Also, the study did not include filtration, such as MERV 8, in the recirculation system. The study was more focused on trade-offs between ventilation and the upper UVGI system. When considering filter efficiencies of MERV 8 (25% for a 1-micron particle and 50% for a 10-micron particle (Zaatari, Novoselac, and Siegel 2014)) and recirculate air flow rates between 0 and 5.3 h^{-1}, the effects of the filter on the removal of viral aerosols may be marginal compared to the removal by the upper room UVGI system.

The exhaled air speed of the infector in the CFD model was set to 2 m/s to approximate human talking. When the infector sneezes or coughs, the air jet velocity leaving the mouth can increase up to 10 m/s and the total output of infectious aerosol also increases (Johnson et al. 2011). In this case, the momentum of the air jet from the mouth has a greater impact on its initial trajectory, influencing the aerosol dispersion characteristics and performance of the UVGI system. For example, experimental studies have shown that the jet produced by a sneeze may still be coherent as much as 8 m away from the source.

CONCLUSIONS

This study examined the transportation of viral aerosol around occupants and the effects of upper-room UVGI on viral species disinfection. Parametric analysis with twelve cases was conducted under representative indoor environmental conditions (ventilation strategies, operation of UVGI, and amount of supply air). The following are the main findings.

1) The exhaled air containing the virus emitted by an infector moved outward and upward due to buoyancy and momentum, then dispersed into the bulk air of the room. The viral particles from the human mouth moved into the UV disinfection zone and were inactivated rapidly before dispersing to the bulk air. Consequently, viral species were confined to a region near the infector, reducing the average room concentrations two orders of magnitude lower than cases without UVGI.

2) The performance of upper room UVGI was affected by both the recirculation rate and ventilation strategy. Mixing ventilation with a higher recirculation rate of indoor air increases UV light exposure on viral aerosol, resulting in lower viral aerosol concentration at the breathing zone.

3) With minimum outdoor air flow and with no recirculation, the average room concentrations under mixing ventilation was 30% lower than for displacement ventilation under the UVGI operation condition

4) The well-mixed model does not consider the effects of airflow on UVGI performance, so this model is not appropriate to estimate the inactivation rate of the UVGI system.

NOMENCLATURE

ϱ = density (kg/m3)
u_j = air velocity (m/s)
M_i = concentration of viral aerosol ($\mu g/m^3$)
D_i = molecular diffusion coefficient
S_i = source term ($\mu g\ h^{-1}$)
R_i = sink term by UVGI inactivation ($\mu g\ h^{-1}$)
I = UV fluence ($\mu w/cm^2$)
k = Susceptibility constant for corona virus ($cm^2/\mu w$)
C_{avg} = a room average concentration of viral aerosol ($\mu g/m^3$)
L = volume (liter)
S = generation rate of viral aerosol (kg/m^3-s)
v = room volume (m^3)
a = air change rate (h^{-1})
γ = the ratio of the volume of the UVGI zone to the volume of the room
W = power of radiance flux (w)
$kI\gamma$ = the equivalent air change of the UVGI (h^{-1})
P2 = people 2
P3 = people 3
P4 = people 4

REFERENCES

ASHRAE, "*ANSI/ASHRAE Standard 62.1-2019. Ventilation for acceptable indoor air quality.*" 2019, American Society of Heating, Refrigerating, and Air-Conditioning Engineers, Inc.: Atlanta, GA

Chao, C.Y.H., M.P. Wan, L. Morawska, G.R. Johnson, Z.D. Ristovski, M. Hargreaves, K. Mengersen, et al. 2009. "Characterization of Expiration Air Jets and Droplet Size Distributions Immediately at the Mouth Opening." *Journal of Aerosol Science* 40 (2): 122–33. https://doi.org/10.1016/j.jaerosci.2008.10.003.

Gupta, Jitendra K., Chao-Hsin Lin, and Qingyan Chen. 2010. "Characterizing Exhaled Airflow from Breathing and Talking." *Indoor Air* 20 (1): 31–39. https://doi.org/10.1111/j.1600-0668.2009.00623.x.

Hult, E. L., H. Willem, P. N. Price, T. Hotchi, M. L. Russell, and B. C. Singer. 2015. "Formaldehyde and Acetaldehyde Exposure Mitigation in US Residences: In-Home Measurements of Ventilation Control and Source Control." *Indoor Air* 25 (5): 523–35. https://doi.org/10.1111/ina.12160.

Johnson, G. R., L. Morawska, Z. D. Ristovski, M. Hargreaves, K. Mengersen, C. Y. H. Chao, M. P. Wan, et al. 2011. "Modality of Human Expired Aerosol Size Distributions." *Journal of Aerosol Science* 42 (12): 839–51. https://doi.org/10.1016/j.jaerosci.2011.07.009.

Kowalski, Wladyslaw. 2010. *Ultraviolet Germicidal Irradiation Handbook: UVGI for Air and Surface Disinfection*. Springer science & business media.

Menter, F. R. 1994. "Two-Equation Eddy-Viscosity Turbulence Models for Engineering Applications." *AIAA Journal* 32 (8): 1598–1605. https://doi.org/10.2514/3.12149.

Nishiura, Hiroshi, Hitoshi Oshitani, Tetsuro Kobayashi, Tomoya Saito, Tomimasa Sunagawa, Tamano Matsui, Takaji Wakita, MHLW COVID-19 Response Team, and Motoi Suzuki. 2020. "Closed Environments Facilitate Secondary Transmission of Coronavirus Disease 2019 (COVID-19)." *MedRxiv*, April, 2020.02.28.20029272. https://doi.org/10.1101/2020.02.28.20029272.

Noti, John D., Francoise M. Blachere, Cynthia M. McMillen, William G. Lindsley, Michael L. Kashon, Denzil R. Slaughter, and Donald H. Beezhold. 2013. "High Humidity Leads to Loss of Infectious Influenza Virus from Simulated Coughs." *PLoS ONE* 8 (2). https://doi.org/10.1371/journal.pone.0057485.

Nunayon, Sunday S., Hui H. Zhang, and Alvin C. K. Lai. 2020. "A Novel Upper-Room UVC-LED Irradiation System for Disinfection of Indoor Bioaerosols under Different Operating and Airflow Conditions." *Journal of Hazardous Materials* 396 (September): 122715. https://doi.org/10.1016/j.jhazmat.2020.122715.

Prather, Kimberly A., Chia C. Wang, and Robert T. Schooley. 2020. "Reducing Transmission of SARS-CoV-2." *Science* 368 (6498): 1422–24. https://doi.org/10.1126/science.abc6197.

Riley, Richard L., and Edward A. Nardell. 1990. "Clearing the Air: The Theory and Application of Ultraviolet Air Disinfection: Reply." *American Review of Respiratory Disease* 142 (5): 1233–34. https://doi.org/10.1164/ajrccm/142.5.1233a.

Shiraiwa, Manabu, Nicola Carslaw, Douglas J. Tobias, Michael S. Waring, Donghyun Rim, Glenn Morrison, Pascale S. J. Lakey, et al. 2019. "Modelling Consortium for Chemistry of Indoor Environments (MOCCIE): Integrating Chemical Processes from Molecular to Room Scales." *Environmental Science: Processes & Impacts* 21 (8): 1240–54. https://doi.org/10.1039/C9EM00123A.

Whalen, John. J. 2009. "Environmental Control for Tuberculosis; Basic Upper-Room Ultraviolet Germicidal Irradiation Guidelines for Healthcare Settings Guide." 2009. https://stacks.cdc.gov/view/cdc/5306.

"WHO Coronavirus (COVID-19) Dashboard." n.d. Accessed April 16, 2021. https://covid19.who.int.

Xu, Jiayao, Han Jiang, Haoran Zhao, and Brent Stephens. 2017. "Mobile Monitoring of Personal NOx Exposures during Scripted Daily Activities in Chicago, IL." *Aerosol and Air Quality Research* 17 (8): 1999–2009. https://doi.org/10.4209/aaqr.2017.02.0063.

Zaatari, Marwa, Atila Novoselac, and Jeffrey Siegel. 2014. "The Relationship between Filter Pressure Drop, Indoor Air Quality, and Energy Consumption in Rooftop HVAC Units." *Building and Environment* 73 (March): 151–61. https://doi.org/10.1016/j.buildenv.2013.12.010.

Zhang, Z., and Q. Chen. 2009. "Prediction of Particle Deposition onto Indoor Surfaces by CFD with a Modified Lagrangian Method." *Atmospheric Environment* 43 (2): 319–28. https://doi.org/10.1016/j.atmosenv.2008.09.041.

Zhu, Shengwei, Jelena Srebric, Stephen N. Rudnick, Richard L. Vincent, and Edward A. Nardell. 2014. "Numerical Modeling of Indoor Environment with a Ceiling Fan and an Upper-Room Ultraviolet Germicidal Irradiation System." *Building and Environment* 72 (February): 116–24. https://doi.org/10.1016/j.buildenv.2013.10.019.